

An ONIOM Study of a Guanidinium Salt Ionic Liquid. Experimental and Computational Characterization of *N,N,N',N',N''*-Pentabutyl-*N''*-benzylguanidinium Bromide

Masato Tanaka^a, Hans-Ullrich Siehl^a, Tillmann Viehhaus^b, Wolfgang Frey^c,
and Willi Kantlehner^{b,c}

^a Institut für Organische Chemie I, Universität Ulm, Albert-Einstein-Allee 11, D-89069 Ulm,
Germany

^b Institut für Organische Chemie der Universität Stuttgart, Pfaffenwaldring 55, D-70569 Stuttgart,
Germany

^c Hochschule Aalen Technik und Wirtschaft, Fakultät Chemie, Beethovenstraße 1, D-73430 Aalen,
Germany

Reprint requests to Hans-Ullrich Siehl. E-mail: Ullrich.siehl@uni-ulm.de

Z. Naturforsch. **2009**, *64b*, 765–772; received May 11, 2009

Dedicated to Professor Gerhard Maas on the occasion of his 60th birthday

The guanidinium salt-based ionic liquid *N,N,N',N',N''*-pentabutyl-*N''*-benzyl-guanidinium bromide was synthesized and characterized by ¹H and ¹³C NMR spectroscopy in solution and by single crystal X-ray structure analysis. The MO computational hybrid method of Morokuma and coworkers (ONIOM method) is applied to compare experimental and quantum chemical results. Four calculation models for two layer ONIOM calculations are defined based on differences of the area for the high-level layer region. Optimized geometries, interaction energies between the cation and the anion, and atomic charges are compared to data of full-QM calculations for the optimized geometry as well as of an experimental X-ray structure determination. The results indicate that it is mandatory for obtaining reasonable results that the parts of the substituent groups which are directly bound to the amino nitrogen atoms are included into the high-level layer. This least required ONIOM model for guanidinium-type ionic liquids can save computational cost of 90 % compared to the full-QM SCF calculation.

Key words: Guanidinium Salts, Ionic Liquids, X-Ray Crystallography, NMR Chemical Shift Calculations, ONIOM Calculations

Introduction

Recently ionic liquids (ILs) have attracted considerable interest because of their potential broad range of applications in various areas of natural and engineering sciences [1]. The physical properties of ILs depend on the substituent groups of the cations as well as on the combination of cations and anions. The large variety of combinations of ionic species and substitution patterns allows the design of ILs with on-demand properties. Guanidinium-based salts are a relatively new class of IL with six substitution sites available in the cation (Fig. 1) which allow a particular broad variation for tailoring the desired functions and properties.

Computational methods such as quantum mechanical (QM) calculations are contemporary established

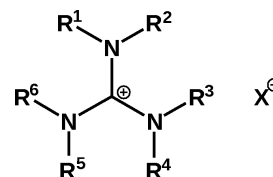


Fig. 1. General formula of guanidinium-based salts.

tools widely used to aid in the design of pharmaceutical drugs and other materials. However, sometimes the system size tempers the applicability of QM methods. For guanidinium ion-based ILs with various multiple substituent groups screening studies with QM calculations would be somewhat time-consuming, thus faster but still accurate methods are desirable. Recently, Morokuma *et al.* have developed a hybrid

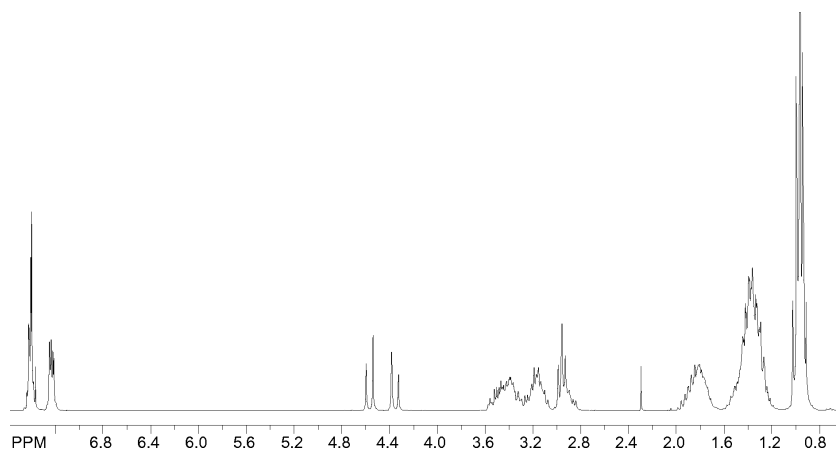
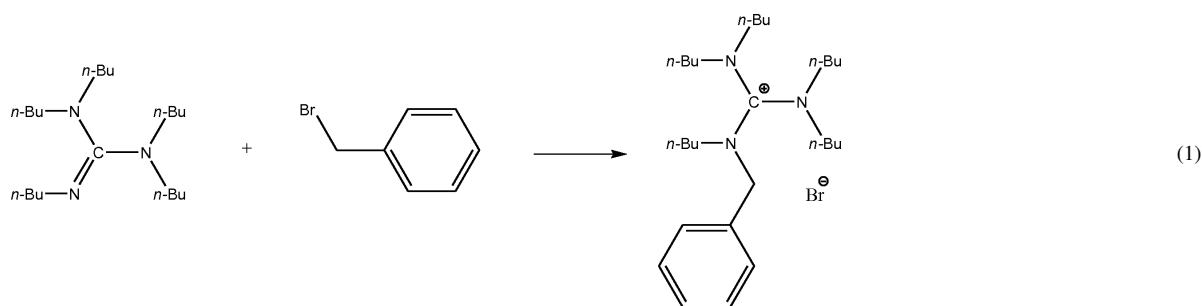


Fig. 2. 250 MHz ^1H NMR spectrum (CDCl_3) of N,N,N',N',N'' -pentabutyl- N'' -benzylguanidinium bromide ($\delta_{\text{TMS}} = 0$ ppm).

method (ONIOM method) [2] to treat large systems using QM calculations. The molecular system is divided into several layers, and a different calculation level is used for each layer depending on the importance. For example, for an enzyme, the active sites are treated with a high-level QM method, and remaining residues are treated with lower-level calculation methods, such as semi-empirical methods or molecular mechanics. This hybrid method is considered to be applicable to computationally investigate substitution effects at reduced cost by using different calculation levels for the main part and the substituent groups of the compounds under investigation. Thus it can be envisaged that the ONIOM method is suitable for screening investigations of guanidinium-based ILs.

In this study, the ONIOM method is applied to a guanidinium-based ionic liquid and compared to full QM calculations to confirm the usability of this approach for the prediction of ILs properties. N,N,N',N',N'' -Pentabutyl- N'' -benzylguanidinium bromide has been synthesized and fully characterized and was chosen as a prototype IL because experimental structural data from single crystal X-ray crystallography could be obtained.

Synthesis

N,N,N',N',N'' -Pentabutyl- N'' -benzylguanidinium bromide was synthesized by reaction of N,N,N',N',N'' -pentabutylguanidine with benzylbromide for 2 h at 60 °C (Eq. 1).

The purified salt was characterized by elemental analysis, IR, and ^1H and ^{13}C NMR spectroscopy in CDCl_3 , and by single crystal X-ray structure determination (details see Experimental Section). The methylene protons of the benzylic group at $\delta = 4.36$ and 4.57 ppm are magnetically non-equivalent and show a geminal spin-spin coupling constant of $^2J_{\text{H,H}} = 14$ Hz (Fig. 2).

Computational Details

The two-layered ONIOM (ONIOM2) method [1] is used to compare the accuracy of the defined layers for the molecule. Four types of ONIOM2 models (ONIOM-I–IV) are defined by relating increasing regions of the molecule to the high-level layer, as shown in Fig. 3. For comparison the whole molecule is investigated by a normal QM calculation, denoted as full-QM. B3LYP/6-31G* is used for the high-level layer,

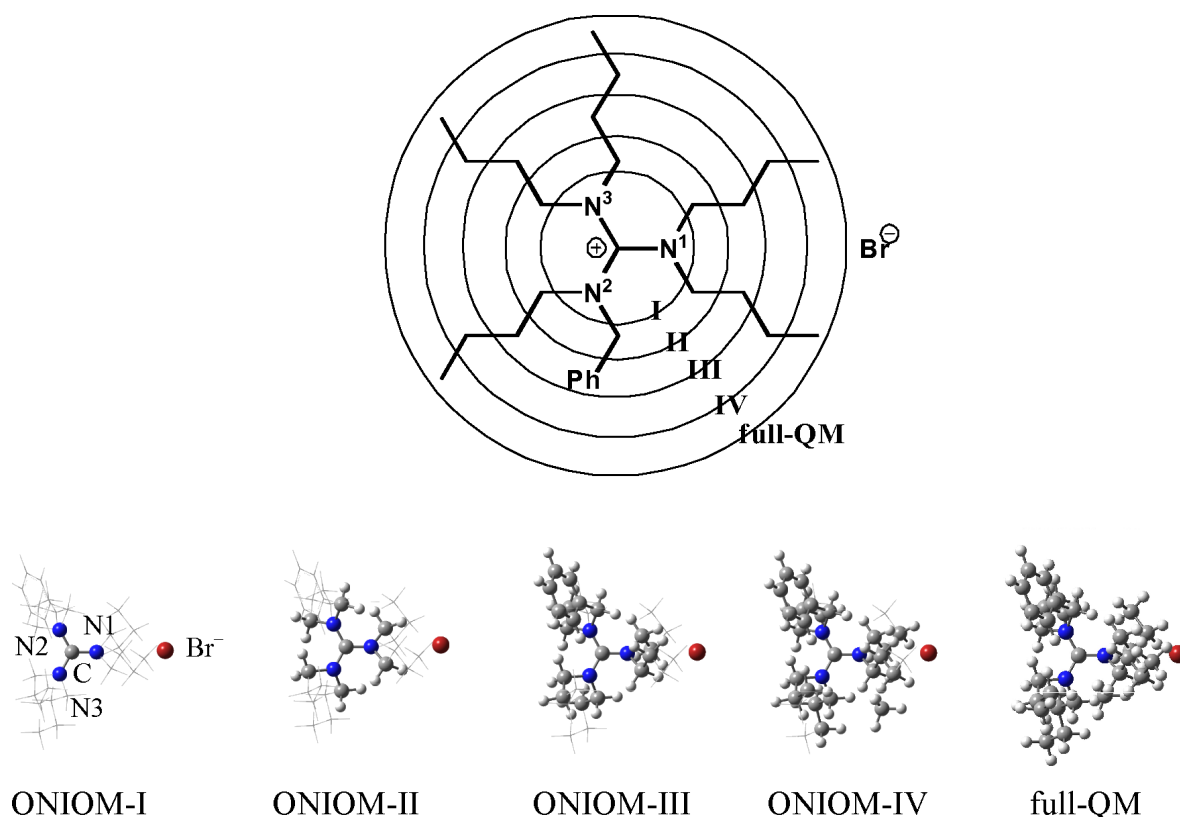


Fig. 3. Four ONIOM2 models (ONIOM-I–IV) and the full-QM model for *N,N,N',N',N''*-pentabutyl-*N''*-benzylguanidinium bromide. The circles confine the regions for four high-level layers in the ONIOM I–IV models and the full-QM model. The ball & stick models and the stick models show the high-level and the low-level layers for the various models, respectively.

and the molecular mechanics force field UFF [3] or the semi-empirical method PM3 [4] are used for the low-level layer calculations. The carbon atoms located at the boundary of layers (link atoms) are treated as hydrogen atoms for the high-level region. The geometry optimization calculations are performed for the four ONIOM2 and the full-QM models, starting from the structural data taken from the X-ray crystal structure study. Normal vibrational mode analyses are performed for the optimized structures to confirm that those are energy minimum structures for each model. The structures optimized by ONIOM2 model calculations are compared with the optimized structure obtained by the full-QM calculation as well as with the experimental data. The program PROFIT [5] is used to obtain the root mean square deviation (RMSD) of structural differences. The atomic charges are also compared. In the charge calculations, only the atoms in the high-level layer are used. The input for the model structures used for the charge calculations are obtained

by replacing the link atoms spanning the QM and the low-level region with hydrogen atoms, deleting the atoms of the low-level layer, and optimizing only the added hydrogen atoms with constraints for the remaining part. The natural charge scheme is used for the atomic charge calculations [6]. The quantum chemical calculations were performed with the GAUSSIAN 03 program suite [7].

Results and Discussions

Optimized structures

The optimized structures obtained by ONIOM2 and full-QM calculations and the experimental molecular structure obtained by single-crystal X-ray diffraction are shown in Fig. 4. The differences of structural parameters and RMSDs are listed in Table 1 and Table 2. The differences between ONIOM2 models and the full-QM model are reduced with increasing circumference of the high-level layer defining the

Table 1. Average differences of structural parameters and root mean square deviations (RMSD) of several ONIOM2 calculations compared to the full-QM calculation.

	ONIOM-I	ONIOM-II	ONIOM-III	ONIOM-IV
High level: B3LYP/6-31G*; Low level: UFF				
Bond length ^a	0.038(0.000/0.135)	0.044(0.000/0.894)	0.035(0.000/1.051)	0.020(0.000/0.116)
Bond angle ^a	1.235(0.011/7.075)	1.045(0.009/5.870)	0.917(0.001/4.015)	0.594(0.000/2.685)
Dihedral angle ^a	5.314(0.013/29.221)	6.377(0.002/43.988)	5.094(0.011/42.521)	1.730(0.003/10.897)
RMSD ^b	0.681 [0.678]	0.873 [0.838]	0.704 [0.634]	0.178 [0.172]
High level: B3LYP/6-31G*; Low level: PM3				
Bond length ^a	0.016(0.000/0.283)	0.019(0.001/0.807)	0.008(0.000/0.102)	0.005(0.000/0.070)
Bond angle ^a	0.905(0.002/3.896)	0.858(0.003/4.145)	0.622(0.004/3.440)	0.400(0.004/2.872)
Dihedral angle ^a	5.684(0.015/32.701)	7.223(0.011/44.583)	5.944(0.001/26.807)	3.440(0.000/24.899)
RMSD ^b	0.682 [0.683]	0.919 [0.878]	0.566 [0.557]	0.331 [0.325]

^a Average differences and minimum/maximum differences (values in parentheses) of bond lengths (Å), bond angles (radian), and dihedral angles (radian) are shown; ^b the RMSDs of the whole system and of the guanidinium cation only [values in brackets] are shown.

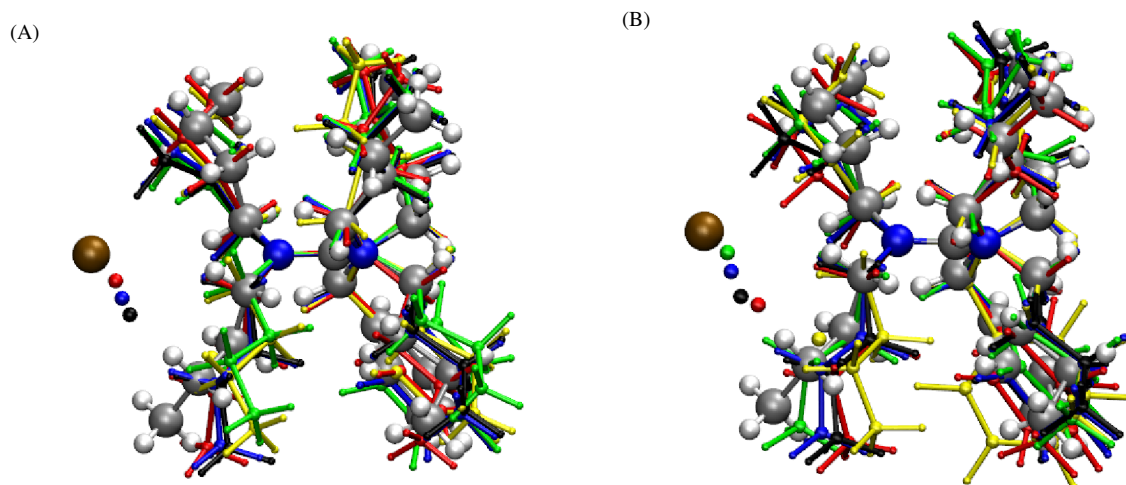


Fig. 4. Comparison of optimized structures. (A) B3LYP/6-31G*:UFF, (B) B3LYP/6-31G*:PM3. The large ball & stick model shows the molecular structure obtained by single-crystal X-ray diffraction, and the red, yellow, green, blue and black models show the structures obtained by ONIOM-I, II, III, IV and full-QM model calculations, respectively (color online).

atoms for QM calculations, except for the ONIOM-I model (Table 1). The ONIOM-I model, with all substituent groups treated at low level, accidentally has a better agreement with the full-QM structure than the ONIOM-II or -III models. There is no significant difference between UFF and PM3 for the low-level layer calculations (Table 1). The differences between several models and the data of the X-ray structure determination (Table 2) are larger than between ONIOM2 models and the full-QM model (Table 1). Even the full-QM model of the optimized structure exhibits some deviations from the experimental X-ray structure data (Table 2). The $C^+ \cdots Br^-$ distance, the $C^+-N1 \cdots Br^-$ angle, and the $N2-C^+-N3 \cdots Br^-$ dihedral angle are 5.24 Å, 155.1°, and -159.7°, respectively, for the full-QM model, and 5.87 Å, 178.0°,

and -178.9°, respectively, for the X-ray data (see Fig. 3 for the numbering of atoms). Thus basically the Br^- anion is located close to the alkyl groups in both the ONIOM2- and the full QM-models and in the experimental X-ray structure without significant differences. The position of the bromide ion is somewhat different depending on the calculational model used (Fig. 3). This in turn leads to conformational changes for the alkyl groups close to the bromide anion. Conversely, if the conformations of alkyl groups change to become more compact, the Br^- anion is in closer distance to the C^+ carbon atom. The RMSDs for the cations only are somewhat smaller than those for the whole ion pair, which is in accord with different relative positions of the bromide anion and the guanidinium cation for the different calculation models. In

Table 2. Average differences of structural parameters and root mean square deviations (RMSD) of several ONIOM2 calculations^a and comparison with the X-ray structure data.

	ONIOM-I	ONIOM-II	ONIOM-III	ONIOM-IV
High level: B3LYP/6-31G*; Low level: UFF				
Bond length ^b	0.077(0.001/0.529)	0.089(0.001/1.527)	0.099(0.001/1.684)	0.086(0.005/0.586)
Bond angle ^b	1.658(0.002/13.641)	1.695(0.005/13.636)	1.850(0.000/13.832)	1.765(0.060/14.373)
Dihedral angle ^b	9.258(0.011/84.978)	11.552(0.079/79.898)	12.305(0.014/81.269)	9.640(0.068/82.009)
RMSD ^c	0.624 [0.624]	1.056 [0.977]	1.119 [1.024]	0.586 [0.579]
High level: B3LYP/6-31G*; Low level: PM3				
Bond length ^b	0.116(0.010/0.916)	0.119(0.006/1.441)	0.106(0.003/0.532)	0.105(0.006/0.563)
Bond angle ^b	1.962(0.023/13.210)	1.990(0.033/13.199)	1.954(0.074/13.558)	1.956(0.006/13.484)
Dihedral angle ^b	10.644(0.079/88.589)	11.723(0.023/77.213)	8.726(0.028/69.243)	9.368(0.083/78.783)
RMSD ^c	0.824 [0.804]	1.155 [1.074]	0.476 [0.474]	0.498 [0.494]

^a A comparison with full-QM calculation results of bond length^b, bond angle^b, dihedral angle^b, and RMSDs^c gives 0.103(0.000/0.633), 1.868(0.003/15.212), 10.217(0.009/84.158), and 0.637 [0.622], respectively; ^b average differences and minimum/maximum differences (values in parentheses) of bond lengths (Å), bond angles (radian), and dihedral angles (radian) are shown; ^c the RMSDs of the whole system and of the guanidinium cation only [values in brackets] are shown.

	ONIOM-I	ONIOM-II	ONIOM-III	ONIOM-IV	full-QM
B3LYP/6-31G*:UFF	-71.0	-79.3	-79.2	-82.9	
B3LYP/6-31G*:PM3	-80.9	-78.2	-79.8	-82.5	-82.5

^a $\Delta E = E(\text{complex}) - E(\text{cation}) - E(\text{anion})$ in kcal mol⁻¹ with the optimized structure of full-QM. The full-QM calculation is done by B3LYP/6-31G*.

the crystal the ordering of cations and anions is governed by additional packing restraints, and thus it is expected that the position of the anion in a single ion pair is different from the position of the anion in the crystal structure.

Interaction energy between the cation and the anion

Table 3 shows a comparison of the interaction energy between the guanidinium ion and the bromide ion calculated with the ONIOM2 and with the full-QM models.

The interaction energy of -82.5 kcal mol⁻¹ obtained by a full-QM calculation is reasonably reproduced by the ONIOM2 calculations within a deviation of ~3 kcal mol⁻¹, except for the ONIOM-I model with UFF. At least the -CH₂- moiety of the alkyl substituents which is linked to the amino nitrogen atoms of the parent guanidinium cation should be included in the high-level layer (ONIOM-II) to obtain reasonable energies compared with the full-QM calculation.

Atomic charges

Table 4 shows the atomic charges for the main atoms in the guanidinium bromide, *viz.* the central carbon (C), the three amino nitrogen (N), and the bromine (Br) atoms, calculated using the ONIOM-I–IV models. The atomic charges calculated for the ONIOM-I model

Table 3. Comparison of interaction energy (ΔE)^a between the cation and the anion.Table 4. Natural atomic charges for main atoms in each model^a.

Atom	ONIOM-I	ONIOM-II	ONIOM-III	ONIOM-IV	full-QM
C	0.681	0.699	0.708	0.707	0.712
N1 ^b	-0.792	-0.420	-0.423	-0.418	-0.409
N2 ^b	-0.821	-0.459	-0.451	-0.458	-0.463
N3 ^b	-0.827	-0.461	-0.468	-0.459	-0.460
Br	-0.905	-0.895	-0.877	-0.872	-0.874

^a Atomic charges for all models are calculated on the B3LYP/6-31G* level; ^b N1: the amino group nearest to the anion; N2: the amino group bearing the benzyl group; N3: the remaining amino group.

differ significantly from those obtained by the full-QM model, in particular for the nitrogen atoms which show almost twice the negative charge in ONIOM-I calculations. It is noteworthy that the atomic charges are almost converged using the ONIOM-II model. Thus the chain link moiety of the substituent groups directly bonded to the amino nitrogen atoms play an important role in describing the charge distribution in the main part of the molecule. This trend is similar to that of the interaction energy as mentioned above. Similar trends are observed for the Mulliken charge definition (data are not shown).

¹³C NMR chemical shifts

The ONIOM-I model gives completely different results compared to full-QM calculations for the central carbon (N₃C⁺), for which the chemical shift is almost converged at ONIOM-III model. The calculated chem-

Table 5. Comparison of ^{13}C NMR chemical shifts from computational^a and experimental data.

	ONIOM-I	ONIOM-II	ONIOM-III	ONIOM-IV	full-QM	exp. ^c
$\text{C}_\delta\text{H}_3$ (Bu) –	–	–	–	–	14.20–16.07 (15.42)	13.30–13.81
$\text{C}_\gamma\text{H}_2$ (Bu) –	–	–	–	12.35–14.68 (13.88) ^b	20.36–23.32 (22.25)	19.99–20.27
C_βH_2 (Bu) –	–	–	13.77–22.03 (16.71) ^b	21.60–29.22 (24.48)	29.53–37.21 (31.86)	29.48, 29.54
$\text{C}_\alpha\text{H}_2$ (Bu) –	–	39.36–45.46 (41.74) ^b	43.27–49.80 (45.11)	48.65–54.00 (51.09)	48.05–52.33 (50.11)	48.5–50.0
$\text{C}_\alpha\text{H}_2$ (Bn) –	–	41.24 ^b	53.37	53.38	53.34	54.00
CH (Ph) –	–	–	122.08–123.62 (122.87)	122.03–123.84 (122.83)	121.97–123.83	128.64, 129.24
C_α (Ph) –	–	–	127.93	127.99	128.10	133.60
N_3C^+	113.19	158.99	157.37	157.33	156.92	163.76

^a $\delta = \delta(\text{TMS}) - \delta(\text{Ccation})$; Reference $\delta(\text{TMS}) = 189.78$ ppm at B3LYP/6-31G*, T_d symmetry, average values are in parentheses; ^b these are linking atoms at the boundary of the QM-level area and are calculated as CH_3 groups; ^c 62.8 MHz in CDCl_3 .

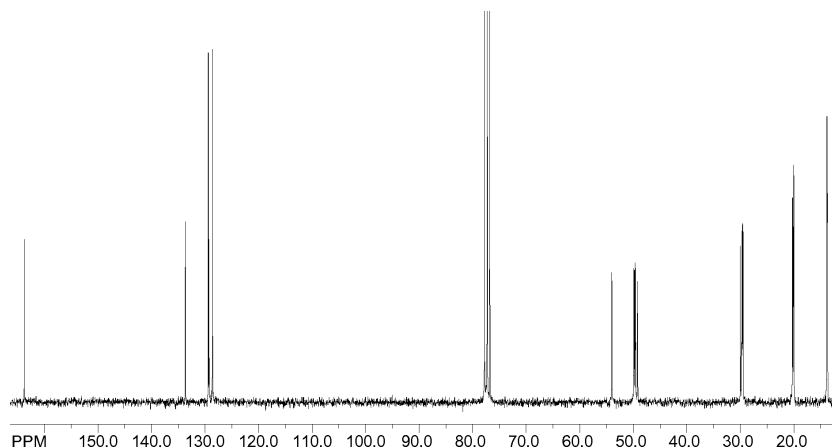


Fig. 5. 62.8 MHz ^{13}C NMR spectrum (CDCl_3) of N,N,N',N',N'' -pentabutyl- N'' -benzylguanidinium bromide ($\delta_{\text{TMS}} = 0$ ppm).

Table 6. Calculation time for QM calculations (High level: HF/6-31G*).

	ONIOM-I	ONIOM-II	ONIOM-III	ONIOM-IV	Full-QM
t , sec ^a	12	556	3432	4988	5416
$\langle t \rangle$, sec ^b	1	37	229	333	602
SCF cycle	13	15	15	15	9

^a Computation time for single point calculation; ^b computation time for one SCF cycle: $\langle t \rangle = t/(\text{number of SCF cycles})$.

ical shifts for the geometry calculated with the full-QM method is in reasonably good agreement with experimental data (Fig. 5 and Table 5).

It is noticeable that calculated chemical shifts are lower than the experimental ones. In addition, carbon atoms located near the bromide anion are less shielded and resonate at relatively high field.

Computation times

The advantage of ONIOM methods in terms of computation costs is shown in Table 6, where the computation times for single point calculations are compared for ONIOM-I–IV models and full-QM calculations. For our model system the computation time for the

low-level calculation for all four ONIOM2 models is negligible (< 1 sec for UFF, and ~ 2 sec for PM3). Thus the gain of using the ONIOM method is due to the reduction of the number of atoms which are treated with high-level QM calculation. The ONIOM-II model which is the least required model for this type of molecules saves 90 % of the computation cost compared to the full-QM calculation.

Conclusions

The ONIOM2 method has been applied to a guanidinium-based ionic liquid. It is shown that a QM treatment of the first chain link which is bonded to the nitrogen atoms is required to obtain results for the interaction energy, geometry and atomic charges which are comparable to full-QM calculations. No obvious difference between UFF and PM3 treatment of the low-level layer was found in this system. The application of our ONIOM-II model is a significant advantage for further screening studies for the design of guanidinium-based ionic liquids which requires the treatment of larger ensembles of ion pair cluster systems.

Table 7. Crystal data and parameters related to the structure determination.

Empirical formula	C ₂₈ H ₅₂ BrN ₃
<i>M_r</i>	510.64
<i>T</i> , K	293(2)
Radiation; wavelength, Å	MoK α , 0.71073
Crystal size, mm ³	1.0 × 0.7 × 0.7
Crystal system, space group	triclinic, <i>P</i> $\bar{1}$
<i>a</i> , Å	10.577(3)
<i>b</i> , Å	11.099(3)
<i>c</i> , Å	14.143(4)
α , deg	101.28(2)
β , deg	95.81(2)
γ , deg	102.16(2)
<i>V</i> , Å ³	1574.0(8)
<i>Z</i>	2
ρ_{calc} , Mg m ⁻³	1.077
μ (MoK α), cm ⁻¹	13.23
<i>F</i> (000), e	552
θ range for data collection, deg	1.48–23.00
Limiting indices <i>hkl</i>	0 ≤ <i>h</i> ≤ 11, –12 ≤ <i>k</i> ≤ 11, –15 ≤ <i>l</i> ≤ 15
Measured/independent reflections	4655/4375
Restrained data	196
Refined parameters	344
<i>R</i> 1/ <i>wR</i> 2 [<i>I</i> ≥ 2 σ (<i>I</i>)]	0.0820/0.2013
<i>R</i> 1/ <i>wR</i> 2 (all data)	0.1730/0.2396
Goodness-of-fit on <i>F</i> ²	1.030
$\Delta\rho_{\text{fin}}$ (max/min), e Å ⁻³	0.34/–0.23

Experimental Section

Synthesis of *N,N,N',N',N''*-pentabutyl-*N''*-benzylguanidinium bromide

2.52 mL (21.1 mmol) benzylbromide is slowly added to a stirred solution of 7.17 g (21.1 mmol) *N,N,N',N',N''*-pentabutylguanidine in 25 mL *n*-pentane and subsequently heated to 60 °C for 2 h. The colorless solid product is separated by filtration and dried *in vacuo* at 10⁻² Torr. Further purification is achieved by dissolving the raw product

in acetone and recrystallization at 8 °C. The colorless crystals are dried *in vacuo* at 10⁻² Torr. The first precipitation yields 4.6 g (8.99 mmol; 42.6 %) of pure *N,N,N',N',N''*-pentabutyl-*N''*-benzylguanidinium bromide; m.p. 116 °C. A strict definition of an IL adopts an upper limit for the melting point below 100 °C, the boiling point of water. – IR (ATR): ν = 2956, 2930, 2869, 1530, 1451, 1434, 1375, 1316, 1231, 1168, 1108, 1086, 940, 892, 883, 737, 703, 574 cm⁻¹. – ¹H NMR (250 MHz, CDCl₃): δ = 0.96 (m, CH₃), 1.38 (m, CH₂), 1.8 (m, CH₂), 2.96, 3.17, 3.42 (3 m, CH₂), 4.36 (d, benzyl-CH₂, ²*J*_{H,H} = 14.2 Hz), 4.57 (d, benzyl-CH₂, ²*J*_{H,H} = 14.1 Hz), 7.23, 7.40, 7.42 (m, benzyl). – ¹³C NMR (62.6 MHz, CDCl₃): δ = 13.68, 13.3, 13.76, 13.81 (CH₃), 19.99, 20.03, 20.08, 20.18, 20.27 (CH₂), 29.48, 29.54 (CH₂), 128.64, 129.24, 133.68 (benzyl), 163.76 (N₂C⁺–N). – C₂₈H₅₂BrN₃ (510.64): calcd. C 65.86, H 10.26, N 8.23, Br 15.65; found C 65.82, H 10.19, N 8.15, Br 15.64.

X-Ray structure determination

A suitable single crystal was obtained by recrystallization from acetone. Diffractometer: Nicolet P3. Structure solution by Direct Methods (SHELXS-97 [8]) and refinement by full-matrix least-squares methods on *F*² (SHELXL-97 [9]). Crystal data and parameters related to the structure determination are summarized in Table 7.

CCDC 7336312 contains the supplementary crystallographic data for this paper. These data can be obtained free of charge from The Cambridge Crystallographic Data Centre via www.ccdc.cam.ac.uk/data_request/cif.

Acknowledgement

This work was supported by the Bundesministerium für Bildung und Forschung (BMBF); Verbundprojekt: Neuartige ionische Flüssigkeiten als innovative Reaktionsmedien für die technische Organische Chemie (Förderkennzeichen 01RI05176-01RI06184).

- [1] P. Wasserscheid, W. Keim, *Angew. Chem.* **2000**, *112*, 3926–3945, *Angew. Chem. Int. Ed.* **2000**, *39*, 3772–3789; T. Welton, *Chem. Rev.* **1999**, *99*, 2071–2083; P. Wasserscheid, T. Welton, Thomas (Eds.), *Ionic Liquids in Synthesis*, (2nd ed.), Wiley-VCH, Weinheim, **2007**; K. R. Seddon, R. D. Rogers (Eds.), *Ionic Liquids: COILED for Action*, John Wiley & Sons, New York **2009**.
- [2] F. Maseras, K. Morokuma, *J. Comp. Chem.* **1995**, *16*, 1170–1179.
- [3] A. K. Rappé, C. J. Casewit, K. S. Colwell, W. A. Goddard III, W. M. Skiff, *J. Am. Chem. Soc.* **1992**, *114*, 10024–10035.
- [4] J. J. P. Stewart, *J. Comp. Chem.* **1989**, *10*, 209–220.
- [5] A. C. R. Martin, PROFIT; available at <http://www.bioinf.org.uk/software/profit/>.
- [6] A. E. Reed, F. Weinhold, *J. Chem. Phys.* **1983**, *78*, 4066–4073.
- [7] M. J. Frisch, G. W. Trucks, H. B. Schlegel, G. E. Scuseria, M. A. Robb, J. R. Cheeseman, J. A. Montgomery, Jr., T. Vreven, K. N. Kudin, J. C. Burant, J. M. Millam, S. S. Iyengar, J. Tomasi, V. Barone, B. Menonucci, M. Cossi, G. Scalmani, N. Rega, G. A. Petersson, H. Nakatsuji, M. Hada, M. Ehara, K. Toyota, R. Fukuda, J. Hasegawa, M. Ishida, T. Nakajima, Y. Honda, O. Kitao, H. Nakai, M. Klene, X. Li, J. E. Knox, H. P. Hratchian, J. B. Cross, V. Bakken, C. Adamo, J. Jaramillo, R. Gomperts,

- R. E. Stratmann, O. Yazyev, A. J. Austin, R. Cammi, C. Pomelli, J. W. Ochterski, P. Y. Ayala, K. Morokuma, G. A. Voth, P. Salvador, J. J. Dannenberg, V. G. Zakrzewski, S. Dapprich, A. D. Daniels, M. C. Strain, O. Farkas, D. K. Malick, A. D. Rabuck, K. Raghavachari, J. B. Foresman, J. V. Ortiz, Q. Cui, A. G. Baboul, S. Clifford, J. Cioslowski, B. B. Stefanov, G. Liu, A. Liashenko, P. Piskorz, I. Komaromi, R. L. Martin, D. J. Fox, T. Keith, M. A. Al-Laham, C. Y. Peng, A. Nanayakkara, M. Challacombe, P. M. W. Gill, B. Johnson, W. Chen, M. W. Wong, C. Gonzalez, J. A. Pople, GAUSSIAN 03 (revision D.02), Gaussian, Inc., Wallingford CT (USA) **2004**.
- [8] G. M. Sheldrick, SHELXS-97, Program for the Solution of Crystal Structures, University of Göttingen, Göttingen (Germany) **1997**.
- [9] G. M. Sheldrick, SHELXL-97, Program for the Refinement of Crystal Structures, University of Göttingen, Göttingen (Germany) **1997**; see also: G. M. Sheldrick, *Acta Crystallogr.* **2008**, *A64*, 112–122.